Talanta 84 (2011) 1038–1046

Contents lists available at ScienceDirect

Talanta

journal homepage: www.elsevier.com/locate/talanta

Recognition of molecularly imprinted polymers for a quaternary alkaloid of berberine

Chia-Yun Chen [a], Chih-Hung Wang [b], Arh-Hwang Chen [b,*]

[a] Material and Chemical Research Laboratories, Industrial Technology Research Institute, Hsinchu 31040, Taiwan, ROC
[b] Department of Chemical and Materials Engineering, Southern Taiwan University, Tainan 71005, Taiwan, ROC

ARTICLE INFO

Article history:
Received 19 January 2011
Received in revised form 28 February 2011
Accepted 3 March 2011
Available online 12 March 2011

Keywords:
Molecularly imprinted polymer
Quaternary alkaloid
Molecular recognition
Adsorption equilibrium
Solid-phase extraction

ABSTRACT

Selective and affinitive imprinted polymers incorporating a quaternary alkaloid of berberine (BER) were prepared using a non-covalent imprinting method. The results showed that, compared to other imprinted polymers, the polymer AD-10 had not only a higher of the ratio of Q_{MIP}/Q_{BP} for BER adsorption, and but also a larger of the ratio of $Q_{MIP,B}/Q_{MIP,P}$ for BER and palmatine (PAL) adsorptions. Spectrophotometric analysis demonstrated that a 1:1 cooperative hydrogen-bonding complex might be predominating in the pre-polymerization between the BER template and AA monomer. Adsorption experiments of BER on the polymer AD-10 were in accordance with the second-order and Langmuir adsorption models. The *E* value (5.70 kJ/mol) calculated from the Dubinin–Radushkevich model indicated that the adsorption followed a physisorption process. In addition, a Scatchard plot showed a single straight line with an equilibrium dissociation constant (K_D) of 65.80 μmol/L. SPE analyses of a mixture of BER and PAL and the methanol extract from the cortices of *Phellodendron wilsonii* showed that AD-10 had more efficiency, and higher specificity and selectivity for SPE in the concentration and determination of BER and its extraction from natural products.

1. Introduction

Molecular imprinting is an attractive technology used to mimic molecular recognition, as it exhibits high affinity and selectivity toward a target molecule. Molecularly imprinted polymers (MIPs) are synthetically prepared by interaction of a functional monomer with a template in a porogenic solvent, followed by polymerization with a cross-linker in the presence of a free radical initiator. The template is removed from the polymer matrix to form cavities sculpted around the template molecules that are complementary in size, shape, and orientation to those of the template. However, selective recognition by the imprinted polymers is critically based on the strength of interaction between the template and the functional monomer. Hence, the choice of functional monomers is crucial to maintain more stable template–monomer interaction during imprinting process [1,2]. This molecular imprinting technique is exploited extensively in many fields, including chiral resolution [3–7], biosensors [8–10], enzyme catalysis, [11,12], biochemical separation [13], drug delivery [14], and the like. In particular, MIPs are widely used as adsorbents of solid-phase extraction (SPE) in the concentration and determination of drug compounds, and the extraction of active components from natural products [15–22].

Berberine (BER), a quaternary isoquinoline alkaloid, is extracted from a plant that mainly grows in Asia and Europe, for example, *Berberis vulgaris*, *Hydrastis canadensis*, *Coptis chinensis*, *Arcangelisia flava*, and *Berberis aquifolium*. It is an ingredient extracted from the plant Coptidis rhizoma, which has been used for centuries as a traditional Chinese medicinal compound to treat inflammatory diseases. This compound has a wide range of pharmacologic effects, including protective effects from some gastric ulcers [23], and treatment of inflammatory [24], cardiovascular, and lipid- and glucose-related diseases [25,26]. BER possesses antimicrobial activity against some bacterial [27,28] and fungal infections [29]. Extraction of BER from plants, however, is tedious and inefficient because of its poor affinity and selectivity to conventional separation materials. It is thus essential to explore efficient adsorbent materials with high affinity for BER.

In the present work, selective and affinitive MIPs incorporating a quaternary alkaloid of BER were prepared using a non-covalent imprinting method employing acrylamide (AA) and methacrylic acid (MAA) as functional monomers, and ethylene glycol dimethacrylate (EGDMA) as a cross-linker in three different porogens ($CHCl_3$, CH_3OH and DMSO). The imprinted polymers were characterized by Fourier transform infrared (FTIR) spectroscopy, thermogravimetric analysis (TGA), and scanning electron microscopy (SEM). Physical features of the polymers, such as

* Corresponding author. Tel.: +886 6 2533131x6937; fax: +886 6 2432846.
E-mail address: chenah@ms12.hinet.net (A.-H. Chen).

0039-9140/$ – see front matter © 2011 Elsevier B.V. All rights reserved.
doi:10.1016/j.talanta.2011.03.009

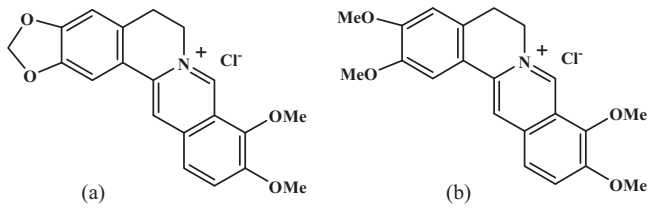

Fig. 1. The molecular structures of (a) BER-CL and (b) PAL-CL.

specific surface areas, pore volumes, and pore diameters, were obtained as well. Recognition and selectivity properties were determined by ultraviolet/visible titration spectroscopy, kinetic and equilibrium adsorption experiments, and isotherm analysis using four models. The optimized imprinted polymer was applied as an adsorbent to extract BER directly from methanol extracts of the cortices of *Phellodendron wilsonii*. The results demonstrated that BER may be directly extracted from plants by using the MIP technology.

2. Experimental

2.1. Materials

Berberine chloride (BER-CL, 95% purity), acrylamide (AA, 97% purity), methacrylic acid (MAA, 99% purity), ethylene glycol dimethacrylate (EGDMA, 98% purity), and 2,2′-azobisisobutyronitrile (AIBN, 98% purity) were purchased from Sigma–Aldrich Company. Palmatine chloride (PAL-CL, 95% purity), acetic acid (CH_3CO_2H), chloroform ($CHCl_3$), dimethyl sulfoxide (DMSO) and methanol (CH_3OH) were supplied by Merck Company. No further purification of the reagents was performed. The structures of BER-CL and PAL-CL are shown in Fig. 1.

2.2. Spectrophotometric analysis of interaction between berberine and monomer

The interaction between the BER template and functional monomers in the solution prior to polymerization was characterized using UV/visible spectrophotometry. The analysis was conducted by titrating a solution of 1.77×10^{-2} mM BER-CL in chloroform with functional monomer solutions (AA and MAA) in the range of 1.77×10^{-2} to 2.12×10^{-1} mM. After equilibrating for 30 min, the changes of absorbance (ΔA) of these solutions were measured at 267 nm using a UV/visible spectrophotometer (Shimadzu UV-2401 PC), with a BER-CL solution as the reference. All experiments were carried out at least twice, and the mean values were used in data analysis.

2.3. Preparation of BER-imprinted polymers

A solution of 0.05 g (0.13 mmol) BER-CL in a glass tube of 6 mL DMSO was added to 0.38 g (5.36 mmol) AA. The solution was aged at room temperature for 4 h in the dark. Subsequently, 9.34 g (53.60 mmol) EGDMA and 33 mg (0.02 mmol) AIBN were added to the solution. The mixture was degassed in a sonicating bath for 10 min and sparged with N_2 for 5 min. The glass tube was sealed and placed in a PanChum multilamp photoreactor, which consisted of 16 Sankyo lamps (8 W, 352 nm lamps), a magnetic stirrer at the center, and a built-in cooling fan at the bottom, for 12 h polymerization. The resultant polymer was ground and then sieved to collect particles with diameters ranging from 37 to 48 μm. Removal of the template from the BER imprinted polymer was performed by Soxhlet extraction. The imprinted polymer was extracted with 100 mL of CH_3OH/CH_3CO_2H (v/v, 9/1) at 120 °C for 12 h. This stage was monitored by a UV/visible spectrophotometer. Afterwards, the polymer, denoted AD-10, was washed intensively with methanol and then dried inside a vacuum oven at 80 °C for 12 h. Non-imprinted polymers were prepared via the same procedure in the absence of the BER template. Eighteen imprinted polymers were prepared through 0.07–0.13 mmol of BER-CL, 2.68–5.36 mmol of the functional monomers (AA and MAA), 26.80–53.60 mmol of cross-linker (EGDMA), and 0.01–0.02 mmol of initiator (AIBN) in 6 mL of three different porogens ($CHCl_3$, CH_3OH, and DMSO), as shown in Table 1.

2.4. Instrumentation

The FTIR spectra of the polymers were obtained using a Perkin Elmer Spectrum One FTIR spectrometer. The TGA curves of the polymers were measured on a Perkin Elmer TGA-7. The specific surface area, pore volume, and pore diameter of the polymers were calculated via the Brunauer–Emmett–Teller (BET) method using a Micromeritics Tristar 3000. SEM photomicrographs of the polymers were taken using a JEOL JSM-6700F scanning electron microscope.

2.5. Adsorption assay

Polymers prepared from different molar ratios of crosslinker/monomer, with or without BER-CL as templates in three different porogens ($CHCl_3$, DMSO and CH_3OH), were studied to determine the adsorption capacity of BER. This process was conducted by adding 20 mg of each of the polymers into

Table 1
Composition of the prepared imprinted polymers.

MIP	Porogen (mL)	BER-CL (mmol)	AA/MAA (mmol)	EGDMA (mmol)	AIBN (mmol)
AC-5	$CHCl_3$ (6.0)	0.13	AA (5.36)	26.80	0.02
AC-10	$CHCl_3$ (6.0)	0.13	AA (5.36)	53.60	0.02
AC-20	$CHCl_3$ (6.0)	0.07	AA (2.68)	53.60	0.01
AD-5	DMSO (6.0)	0.13	AA (5.36)	26.80	0.02
AD-10	DMSO (6.0)	0.13	AA (5.36)	53.60	0.02
AD-20	DMSO (6.0)	0.07	AA (2.68)	53.60	0.01
AM-5	CH_3OH (6.0)	0.13	AA (5.36)	26.80	0.02
AM-10	CH_3OH (6.0)	0.13	AA (5.36)	53.60	0.02
AM-20	CH_3OH (6.0)	0.07	AA (2.68)	53.60	0.01
MC-5	$CHCl_3$ (6.0)	0.13	MAA (5.36)	26.80	0.02
MC-10	$CHCl_3$ (6.0)	0.13	MAA (5.36)	53.60	0.02
MC-20	$CHCl_3$ (6.0)	0.07	MAA (2.68)	53.60	0.01
MD-5	DMSO (6.0)	0.13	MAA (5.36)	26.80	0.02
MD-10	DMSO (6.0)	0.13	MAA (5.36)	53.60	0.02
MD-20	DMSO (6.0)	0.07	MAA (2.68)	53.60	0.01
MM-5	CH_3OH (6.0)	0.13	MAA (5.36)	26.80	0.02
MM-10	CH_3OH (6.0)	0.13	MAA (5.36)	53.60	0.02
MM-20	CH_3OH (6.0)	0.07	MAA (2.68)	53.60	0.01

10 mL of 0.05 mM BER chloroform solution, and then stirring at 30 °C for 12 h. The mixture solution was filtered through Millipore 0.45-μm HV filter paper to remove adsorbents. The filtrate was diluted to 25 mL with chloroform. The BER concentration was measured at 267 nm using a UV/visible spectrophotometer, where the adsorption capacity (Q) was calculated using Eq. (1):

$$Q = \frac{(C_i - C_f)V}{W} \quad (1)$$

where C_i (mM) is the initial concentration of BER; C_f (mM) is the final concentration of BER; V (L) is the volume of dye solution; and W (g) is the weight of the polymers used. All experiments were carried out at least twice, and the mean values were used in data analysis.

2.6. Adsorption kinetics

Analysis of the adsorption kinetics of BER on the imprinted polymer (AD-10) was carried out in a batch process. In each test, 20 mg of AD-10 was placed in 10 mL of 0.05 mM BER chloroform solution. Afterwards, 0.1 mL of the solution at different time intervals was added to 5 mL chloroform. The mixture was filtered through Millipore 0.45 μm HV filter paper, and then diluted to 10 mL with chloroform. The concentrations of BER were measured at 267 nm using a UV/visible spectrophotometer. The adsorption amount was calculated using Eq. (1). All experiments were carried out at least twice, and the mean values were used in data analysis.

2.7. Adsorption equilibrium

The adsorption equilibrium experiment was conducted by adding 20 mg of the imprinted polymer into 10 mL of the initial BER chloroform concentrations within the range of 0.0125–0.25 mM, and then stirring at 30 °C for 12 h. The mixture was filtered through Millipore 0.45 μm HV filter paper, and then diluted to 25 mL with chloroform. BER concentrations were measured at 267 nm using a UV/visible spectrophotometer. The adsorption amount was calculated using Eq. (1). All experiments were carried out at least twice, and the mean values were used in data analysis.

2.8. SPE assay

An SPE column (4 mm × 80 mm) was packed with 0.2 g of AD-10, with a glass-wood frit on top of the polymer. During SPE operation, 0.5 mL of a mixture of 0.1 mm BER-CL and 0.1 mm PAL-CL, or methanol extract from the cortices of *P. wilsonii* were loaded, and then eluted with 3 mL of different volume ratios of methanol and chloroform under an N_2 atmosphere. The eluted solutions were analyzed using the HPLC method with the following conditions: column: μ-Bondpack C18 (3.9 mm × 30 cm, Waters); eluting solution: 3/2 (v/v) of acetonitrile and 1/15 M potassium dihydrogenphosphate–1/15 M sodium hydrogen phosphate buffer (pH 5.2); flow rate: 0.5 mL/min; detector: 267 nm. HPLC analysis was performed on a Jasco HPLC System (PU-2080 Pump, LG-2080-04 Low Pressure Mixer and DG-2080-54 In-line Degasser) with a Waters tunable absorbance detector equipped with an SISC chromatograph. All experiments were carried out at least twice, and the mean values were used in data analysis.

3. Results and discussion

3.1. Interaction between the berberine template and monomers

The recognition properties of the imprinted polymers are greatly affected by the strength and positioning of the interaction between the template and the functional monomer [3,4]. BER is a suitable template to be used in the imprinting process on account of its rigid structure and its good hydrogen-bond acceptor sites with functional monomers, such as AA and MAA. Hence, spectroscopy is a valuable tool for investigating the strength of interaction between the BER template and functional monomers [19,30].

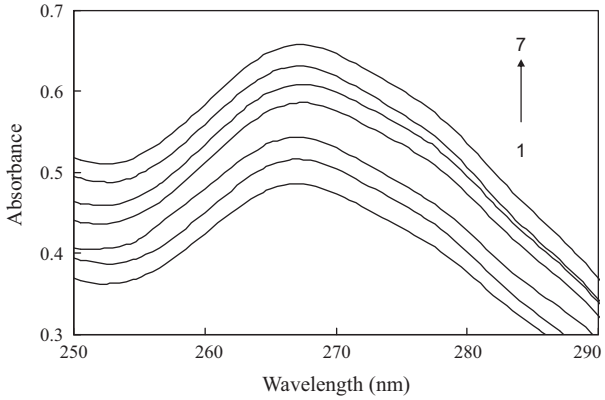

Fig. 2. UV/visible spectra of BER in the presence of different concentrations of AA in $CHCl_3$. Concentration of BER: 1.77×10^{-2} mM; Concentration of AA for lines 1–7: 0, 1.77×10^{-2}, 3.54×10^{-2}, 7.08×10^{-2}, 1.06×10^{-1}, 1.41×10^{-1} and 2.12×10^{-1} mM.

In general, the formation of the complex C between template B and functional monomer B can be expressed by the following reaction, shown as Eq. (2):

$$A + nB \rightarrow C \quad (2)$$

where $n = 1, 2, 3$, etc. is the composition of the complex, and K_a is the association constant.

If the concentration of monomer B (b_0) is much higher than that of template A (a_0), the equilibrium concentration of monomer B is approximated as b_0. K_a can be written as Eq. (3), and then the complex concentration (c) can be calculated by Eq. (4).

$$K_a = \frac{c}{b_0^n(a_0 - c)} \quad (3)$$

$$c = \frac{a_0 b_0^n K_a}{1 + b_0^n K_a} \quad (4)$$

The absorbance of the mixture measured at a given wavelength can be expressed as Eq. (5):

$$A = A_A + A_B + A_C = [(a_0 - c)\varepsilon_A + (b_0 - nc)\varepsilon_B + c\varepsilon_C]l \quad (5)$$

where ε_A, ε_B and ε_C are the molar absorptivities of A, B, and C, respectively, and l is the cell length.

When $b_0 = 0$, the absorbance (A_0) is expressed as Eq. (6):

$$A_0 = a_0 \varepsilon_A l \quad (6)$$

When the absorption is measured at a wavelength that monomer B cannot yield any absorption, the difference in absorbance of the mixture (ΔA) is calculated as in Eq. (7):

$$\Delta A = A - A_0 = c\Delta\varepsilon l \quad (7)$$

where $\Delta\varepsilon = \varepsilon_C - \varepsilon_A$. Substituting Eq. (7) into Eq. (4) yields Eq. (8):

$$\frac{\Delta A}{b_0^n} = -K_a \Delta A + K_a \Delta\varepsilon a_0 l \quad (8)$$

Hence, K_a and n can be obtained by plotting $\Delta A/b_0^n$ versus ΔA.

In this study, spectroscopic analysis was performed in a chloroform solution of 1.77×10^{-2} mM BER-CL with the addition of functional monomer solutions (AA or MMA) in the range of 1.77×10^{-2} to 2.12×10^{-1} mM. After equilibrating for 30 min, the UV/visible spectra of the mixtures were measured, as shown in Fig. 2 for AA. The changes in absorbance (ΔA) of the solutions

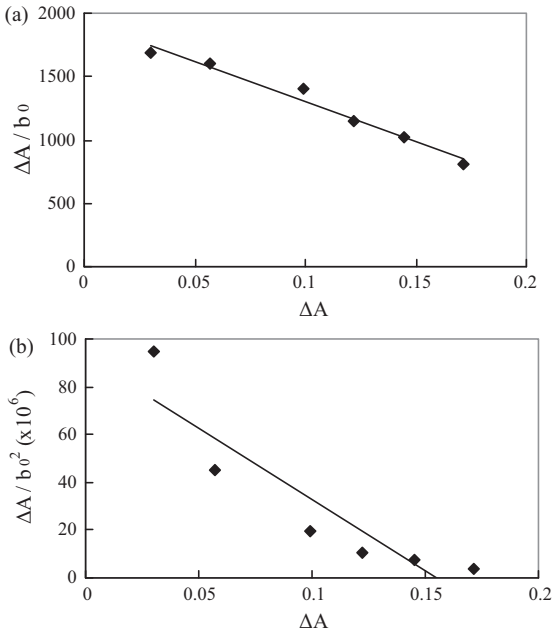

Fig. 3. Plots of (a) $\Delta A/b_0$ versus A and (b) $\Delta A/b_0^2$ versus A at 267 nm for BER in the presence of different concentrations of AA in $CHCl_3$.

were determined at 267 nm, at which AA and MAA cannot produce any absorption, with varying concentrations of AA or MAA. According to Eq. (8), the appropriate plots of $\Delta A/b_0^n$ versus ΔA give straight lines whose slopes are $-K_a$ (Fig. 3 for AA). The data showed that good linear relationships with correction coefficients of 0.9738 and 0.9643 for the monomers AA and MAA, respectively, were obtained at $n = 1$, and the linear regression equations were calculated as $\Delta A/b_0^1 = -6354.9\Delta A + 1937.2$ and $\Delta A/b_0^1 = -54.125\Delta A + 8.7976$ for AA and MAA, respectively. This result indicated that a 1:1 cooperative hydrogen-bonding complex might predominate in the pre-polymerization mixture [19]. In addition, the value of the association constant (K_a) of AA, 6.35×10^3 L/mol, was higher than that of MAA, 5.13×10 L/mol. This reveals that the BER–AA complex was more stable than the BER–MAA complex, which may be ascribed to the fact that the two hydrogen atoms of the amide group in AA have the chance to interact with BER by hydrogen bonds compared to the single hydrogen atom of the carboxylic acid group in MAA. Thus, more stable cyclic hydrogen bonds are formed between BER and AA, as shown in Fig. 4 [19].

3.2. Preparation and characterization

The imprinted polymers were prepared using a non-covalent imprinting method through the following steps: (1) pre-polymerization of the template (BER) and functional monomers (AA or MAA) through hydrogen bonding and ion–dipole and dipole–dipole interactions, (2) polymerization of the functional

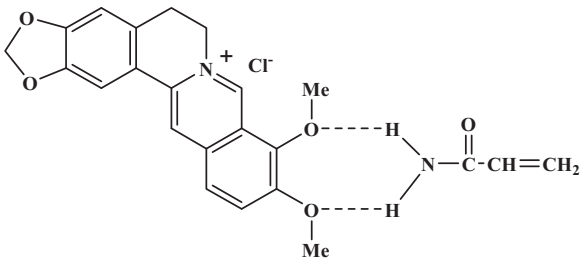

Fig. 4. The proposed structure for hydrogen bonding of BER with AA.

Table 2
Surface area, pore volume and pore diameter of three imprinted polymers.

MIP	Specific surface area (m^2/g)	Pore volume (cm^3/g)	Pore diameter (nm)
AC-10	6.24	0.0036	2.30
AD-10	295.81	0.3762	5.09
AM-10	200.81	0.3061	6.01

monomers (AA or MAA) and cross-linker (EGDMA) with an initiator (AIBN) under irradiation of 352 nm, and (3) removal of the template by Soxhlet extraction with CH_3OH/CH_3CO_2H (v/v, 9/1), as shown in Fig. 5(a) for the AA monomer with BER as a template and EGDMA as a cross-linker. In order to optimize the imprinted system, a series of the imprinted polymers were synthesized with different molar ratios of the functional monomers (AA and MAA) and cross-linker (EGDMA) in three different porogens ($CHCl_3$, CH_3OH, and DMSO), as shown in Table 1. The FTIR spectra of the imprinted polymers showed absorption peaks at 3551 cm^{-1}, assigned to O–H stretching vibrations, 3412 and 3352 cm^{-1}, assigned to N–H stretching vibrations for AA used as a functional monomer, 1717 and 1636 cm^{-1}, assigned to C=O stretching vibrations, and 1237 and 1137 cm^{-1}, assigned to C–O stretching vibrations (Fig. 6) [31]. The thermal decomposition temperatures (T_d) of the imprinted polymers prepared from the AA monomer (269.9–282.2 °C) were found to be higher than those prepared from the MAA monomer (261.8–265.4 °C) (Fig. 7). The results indicated that the imprinted polymers formed from the MAA monomer were more easily decomposed than those formed from the AA monomer. This may be attributed to the decomposition of the carboxylic acid group of the MAA monomer. In addition, the porogen used in the preparation of the imprinted polymers plays an important factor in the morphology of the polymer, influencing the surface morphology [32]. Fig. 8 shows the SEM images of three imprinted polymers, AC-10, AD-10, and AM-10, which were synthesized under the same conditions but with the porogens, $CHCl_3$, DMSO, and CH_3OH, respectively. AM-10, prepared with CH_3OH, showed less density and homogeneity and more irregular cavities than the other polymers. The polymers prepared from the MAA monomer yielded the same results. This may be caused by the association of the functional monomers (AM and MAA) with CH_3OH via hydrogen bonding in pre-polymerization, resulting in the formation of more irregular cavities after polymerization [32]. The results obtained from calculations using the BET method showed that AD-10 had a larger specific surface area (295.81 m^2/g) compared to the other polymers (Table 2). Therefore, the imprinted polymers prepared through AA functional monomer with BER template in DMSO yielded more thermal stability and higher specific surface area.

3.3. Effect of polymerization condition on adsorption property

The most important factors for the affinity and selectivity of imprinted polymers prepared using a non-covalent imprinting method include the complementary interaction between the template and functional monomer, porogenic solvent, and cross-linker, and the polymerization method used [20,30,32]. The strength of intermolecular interactions between the template and functional monomer has an effect on the number and property of MIP recognition sites. However, the interaction between the porogenic solvent and template and/or functional monomer increases with increasing polarity of the solvent, resulting in a decrease in the specific recognition capacity of MIPs. The cross-linker is employed to control matrix stability and the solid shapes of the imprinting binding sites after removal of the template. The polymerization method also influences specific recognition characteristics, as well as the internal and external morphology of the polymer. Table 3 shows

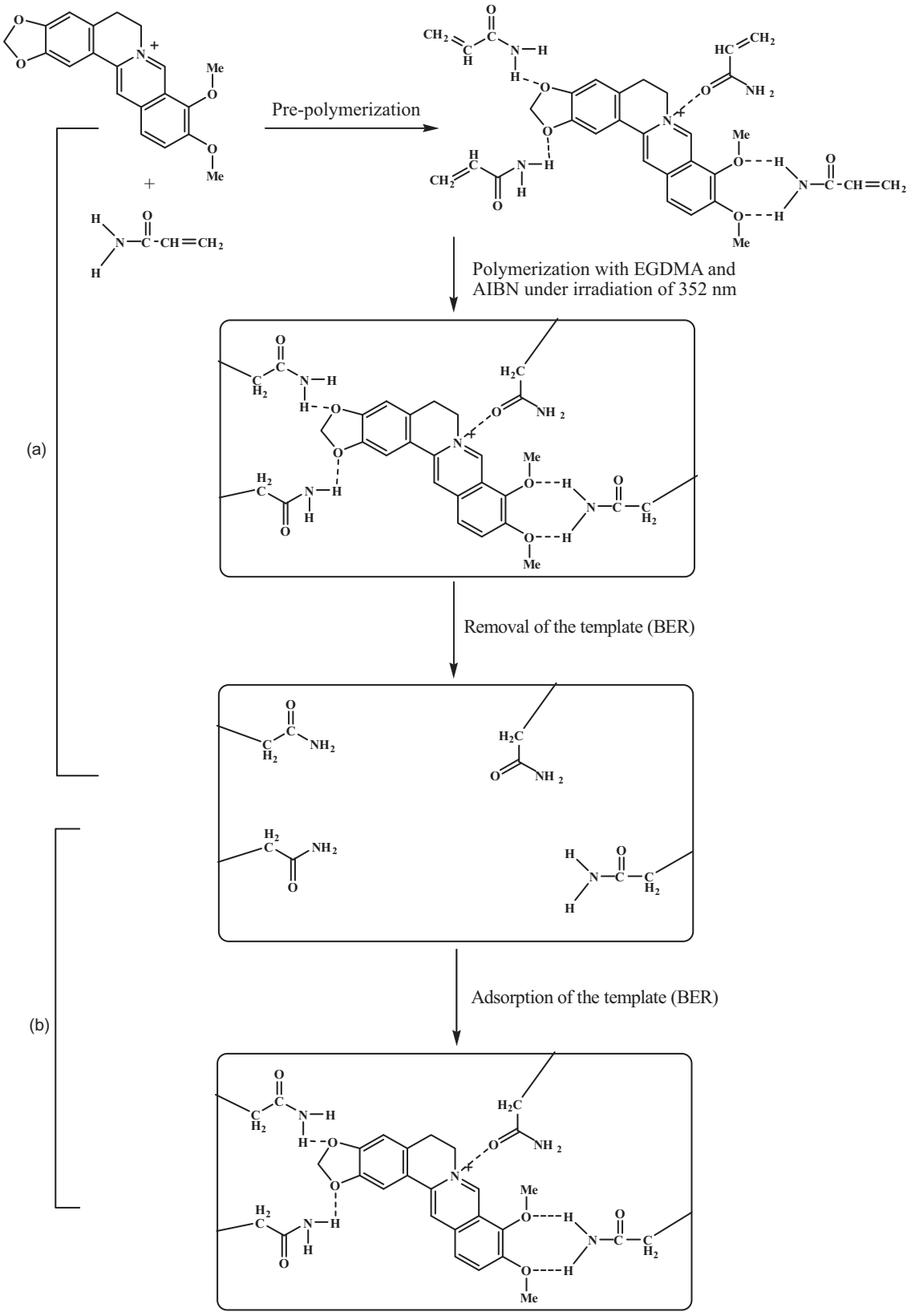

Fig. 5. Schematic representation for (a) preparation of the imprinted polymers of BER as a template and (b) adsorption of the template (BER).

the adsorption capacities of BER on the imprinted (Q_{MIP}) and non-imprinted polymers (Q_{BP}) at 0.05 mM concentration of BER in $CHCl_3$ solution and 30 °C for 12 h. The adsorption process may involve hydrogen-bonding and ion–dipole and dipole–dipole interactions between the berbinium cation, methoxy and methylenedioxy groups of BER and the amide, carboxylic acid, or ester groups of the imprinted polymer, which are dependent on the functional monomers and cross-linkers used (Fig. 5(b)). The results showed

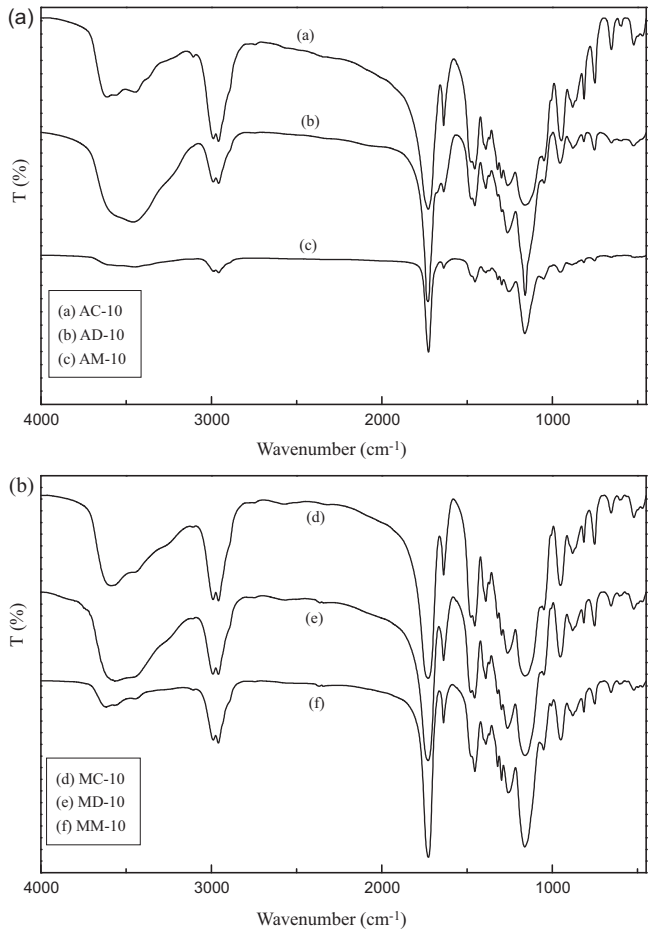

Fig. 6. FTIR spectra of the imprinted polymers: (a) AC-10, (b) AD-10, (c) AM-10, (d) MC-10, (e) MD-10, and (f) MM-10.

that the ratio of adsorption capacities for Q_{MIP} and Q_{BP} of AD-10 (1.91) were much higher than those of the other imprinted polymers. In order to verify the specificity of the imprinted polymers for BER, a comparison of the adsorption capacities of BER and the related compound PAL on six imprinted polymers at 0.05 mM concentration of BER or PAL in $CHCl_3$ solution at 30 °C was evaluated, as

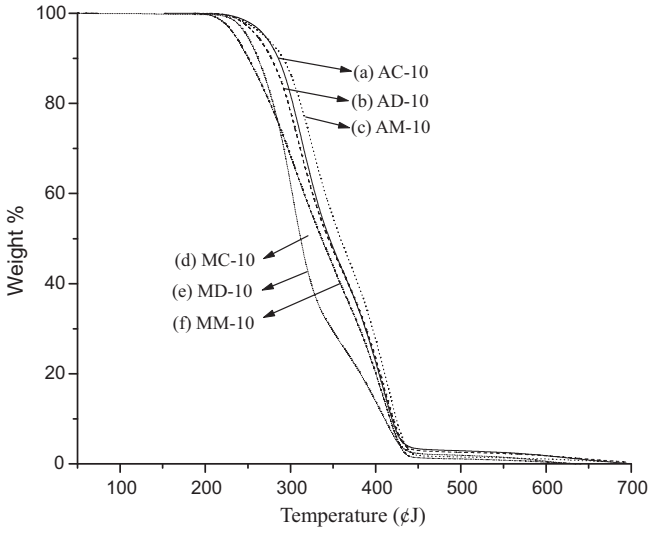

Fig. 7. TGA curves of six imprinted polymers: (a) AC-10, (b) AD-10, (c) AM-10, (d) MC-10, (e) MD-10, and (f) MM-10.

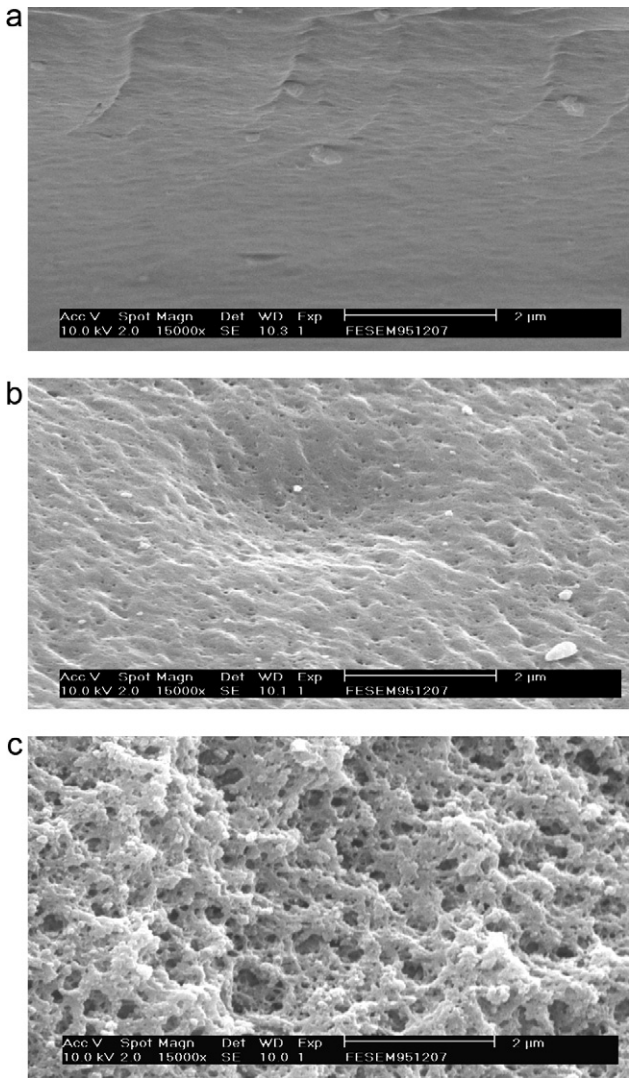

Fig. 8. SEM photomicrographs of three imprinted polymers: (a) AC-10, (b) AD-10, and (c) AM-10.

Table 3
Adsorption capacity of BER on the imprinted polymers (Q_{MIP}) and non-imprinted polymers (Q_{BP}) at 0.05 mM concentration of BER in $CHCl_3$ solution and 30 °C for 12 h.

MIP	Q_{MIP} (μmol/g)	Q_{BP} (μmol/g)	Q_{MIP}/Q_{BP}
AC-5	4.67	3.72	1.26
AC-10	6.90	4.31	1.60
AC-20	5.35	3.86	1.38
AD-5	5.50	4.31	1.28
AD-10	12.80	6.70	1.91
AD-20	5.05	4.31	1.17
AM-5	5.30	3.87	1.37
AM-10	7.68	4.61	1.67
AM-20	5.95	4.46	1.33
MC-5	4.88	3.57	1.37
MC-10	5.86	3.86	1.52
MC-20	4.02	3.57	1.13
MD-5	6.25	5.65	1.11
MD-10	11.90	7.14	1.67
MD-20	5.95	4.02	1.48
MM-5	5.36	3.87	1.39
MM-10	6.16	4.32	1.43
MM-20	3.96	3.04	1.30

Table 4
Comparison for adsorption capacities of BER and PAL on six imprinted polymers at 0.05 mM concentration of BER and PAL in $CHCl_3$ solution at 30 °C.

MIP	$Q_{MIP,B}$ (μmol/g)	$Q_{MIP,P}$ (μmol/g)	$Q_{MIP,B}/Q_{MIP,P}$
AC-10	6.90	1.96	3.52
AD-10	12.80	2.47	5.18
AM-10	7.68	2.33	3.30
MC-10	5.86	2.19	2.68
MD-10	11.90	2.32	5.12
MM-10	6.16	1.73	3.56

Note: $Q_{MIP,B}$ and $Q_{MIP,P}$ are adsorption capacities of BER and PAL, respectively.

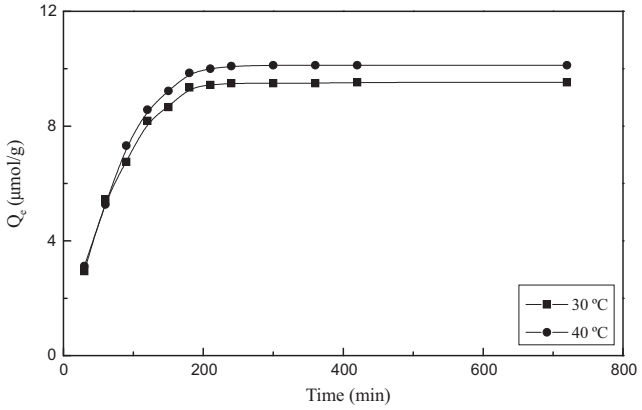

Fig. 9. Adsorption kinetics of BER on the imprinted polymer (AD-10) at 0.05 mM concentration of BER in $CHCl_3$ solution.

shown in Table 4. The results indicated that the adsorption ratios of BER and PAL ($Q_{MIP,B}/Q_{MIP,P}$) on AD-10 (5.18) were larger that those of other polymers. This may be ascribed to the fact that AD-10 from the functional monomer AA and BER template, which forms a 1:1 cooperative hydrogen-bonding complex during pre-polymerization, yielded numerous and precise imprinting sites, and had a larger specific surface area (295.81 m^2/g), resulting in higher ratios of Q_{MIP}/Q_{BP} and $Q_{MIP,B}/Q_{MIP,P}$. The technique for the preparation of AD-10 yielded higher adsorption capacity and more efficient adsorption of BER.

3.4. Adsorption analysis and recognition mechanism

Since AD-10 had higher adsorption capacity and more efficient adsorption of BER than the other imprinted polymers, it was used as an adsorbent for kinetic and equilibrium studies for the adsorption of BER. Fig. 9 shows the dynamic curves of the adsorption of BER onto AD-10 at 0.05 mM concentration of BER in $CHCl_3$ solution at different temperatures (30 and 40 °C). The adsorption capacities of BER increased with time, reaching a nearly saturated state within 240 min. The adsorption capacity of BER increased by only 6.30% with increasing temperature from 30 to 40 °C. The higher adsorption rate observed within 180 min may have resulted from the preferential and rapid adsorption of the BER template onto the recognition sites on the surface of polymer. After the imprinted sites on the surface of the polymer were occupied, it became difficult for

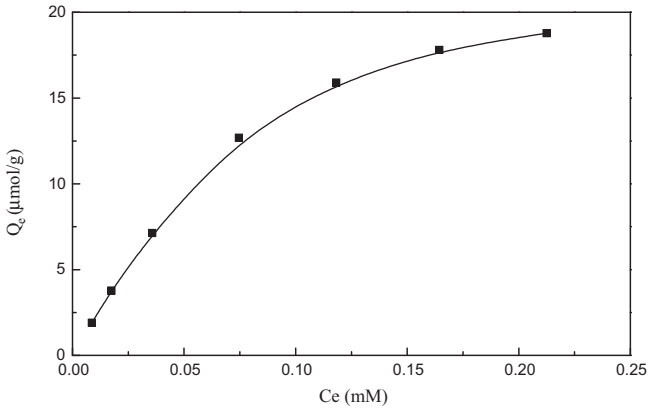

Fig. 10. Adsorption equilibrium of BER on the imprinted polymer (AD-10) at 30 °C for 12 h with different equilibrium concentrations.

BER to implant into the polymer, resulting in slower adsorption [20].

In order to determine the rate-controlling and mass transfer mechanisms, kinetic data were correlated to linear forms of the first-order equation (9),

$$\ln(Q_e - Q_t) = \ln\ Q_e - k_1 t, \tag{9}$$

and the second-order equation (10),

$$\frac{t}{Q_t} = \frac{1}{k_2 Q_e^2} + \frac{t}{Q_e}, \tag{10}$$

where Q_e (μmol/g) and Q_t (μmol/g) are the adsorption capacities of BER at equilibrium and at a given time t, respectively; and k_1 (min^{-1}) and k_2 (g/(μmol min)) are the first-order and the second-order rate constants, respectively. According to Eq. (9), the plot of $\ln(Q_e - Q_t)$ versus t gives a straight line with a slope of $-k_1$ and an intercept of $\ln Q_e$. From Eq. (10), the plot of t/Q_t versus t gives a straight line with a slope of $1/Q_e$ and an intercept of $1/k_2 Q_e^2$.

The dynamic experimental parameters are listed in Table 5. The correlation coefficient (R^2) of the second-order adsorption model exhibited a higher value than that of the first-order model. In addition, the calculated equilibrium adsorption capacity, $Q_{e,cal}$, from the second-order model fitted well with the experimental data, $Q_{e,exp}$. This indicated that the second-order kinetic equation fitted the dynamic experimental data better than that of the first-order kinetics equation.

The experimental equilibrium isotherms for the adsorption of BER onto AD-10 at 30 °C for 12 h with different equilibrium concentrations are shown in Fig. 10. Four different adsorption isotherm models, namely the Langmuir, Freundlich, Dubinin–Radushkevich, and Scatchard isotherm models, were applied.

The Langmuir isotherm model, which is that most commonly used for monolayer adsorption onto a surface with a finite number of identical sites, is represented by Eq. (11) [33]:

$$\frac{C_e}{Q_e} = \frac{C_e}{Q_m} + \frac{1}{Q_m K_L} \tag{11}$$

where C_e (mM) is the equilibrium concentration of BER, Q_e (μmol/g) is the adsorption capacity of BER, Q_m (μmol/g) is the maximum

Table 5
Comparison of the first-order and second-order adsorption rate constants, experimental and calculated Q_e values for adsorption of BER on the imprinted polymer (AD-10).

AD-10		First-order kinetic model			Second-order kinetic model		
T (°C)	Q_e,exp (μmol/g)	k_1 ($\times 10^{-2}$ min^{-1})	Q_e,cal (μmol/g)	R^2	k_2 ($\times 10^{-6}$ g/(μmol min))	Q_e,cal (μmol/g)	R^2
30	9.52	1.92	39.58	0.8819	4.87	11.19	0.9848
40	10.11	2.14	107.08	0.9398	4.22	12.02	0.9833

Note: R^2 is the correlation coefficient.

adsorption capacity of BER, and K_L (L/mmol) is the Langmuir adsorption equilibrium constant. Therefore, the plot of C_e/Q_e against C_e gives a straight line with a slope of $1/Q_m$ and an intercept of $1/(Q_mK_L)$.

The Freundlich isotherm model, the most important multilayer adsorption isotherm for heterogeneous surfaces, is described by Eq. (12) [34]:

$$\ln Q_e = b_F \ln C_e + \ln K_F \quad (12)$$

where C_e (mM) is the equilibrium concentration of BER, Q_e (μmol/g) is the adsorption capacity of BER, K_F is the maximum adsorption capacity of BER (μmol/g), and b_F is the adsorption intensity. K_F and b_F can be determined from a linear plot of $\ln Q_e$ versus $\ln C_e$.

The Dubinin–Radushkevich isotherm model, which is more generally used to distinguish between physical and chemical adsorption, is given by Eq. (13) [35]:

$$\ln Q_e = K\varepsilon^2 + \ln Q_{DR} \quad (13)$$

where Q_e (μmol/g) is the adsorption capacity of BER, Q_{DR} (μmol/g) is the maximum adsorption capacity of BER, K (kJ^2/mol^2) is the Dubinin–Radushkevich constant, and ε is the Polanyi potential, given in Eq. (14):

$$\varepsilon = RT \ln\left(1 + \frac{1}{C_e}\right) \quad (14)$$

where R is the gas constant in J/K mol, T is the temperature in kelvin, and C_e (mM) is the equilibrium concentration of BER. Thus the plot of $\ln Q_e$ against ε^2 gives a straight line with a slope of K and an intercept of Q_{DR}. The Dubinin–Radushkevich constant can give valuable information regarding the mean energy of adsorption using Eq. (15):

$$E = (-2K)^{-1/2} \quad (15)$$

where E (kJ/mol) is the mean adsorption energy, and K is the Dubinin–Radushkevich constant.

The Scatchard isotherm model, which is commonly used to estimate the binding properties of imprinted polymers, can be expressed as Eq. (16) [36]:

$$\frac{Q_e}{C_e} = \frac{Q_{max}}{K_D} - \frac{C_e}{K_D} \quad (16)$$

where C_e (mM) is the equilibrium concentration of BER, Q_e (μmol/g) is the adsorption capacity of BER, Q_{max} (μmol/g) is the apparent maximum adsorption capacity of BER, and K_D (μmmol/L) is the equilibrium dissociation constant. Q_{max} and K_D can be obtained from a linear plot of Q_e/C_e versus C_e.

The model parameters obtained from the four isotherm models are listed in Table 6. The Langmuir adsorption model was found to sufficiently fit the experimental data of BER on AD-10 compared to the other linear correlation coefficients (R^2). Meanwhile, the mean adsorption energy (E) calculated from the Dubinin–Radushkevich model may involve the transfer of the free energy of one mole of the solute from infinity (in solution) to the surface of the adsorbent. The adsorption behavior can predict physical adsorption in the range of 1–8 kJ/mol and chemical adsorption at over 8 kJ/mol [37–39]. The E value (5.70 kJ/mol) of BER indicates that the adsorption followed a physisorption process. The Scatchard plot of BER on AD-10 showed a single straight line with a high correlation coefficient (R^2 = 0.9792); and Q_{max} and K_D were calculated to be 21.45 μmol/g and 65.80 μmol/L, respectively. This suggests that the homogeneous recognition sites for BER are formed in the imprinted polymers [20]. It could be assumed that the adsorption of BER onto the imprinted polymers mainly involves physisorption via hydrogen-bonding and ion–dipole and dipole–dipole interactions between BER and the imprinted polymers.

Table 6
Langmuir, Freundlich, Dubinin–Radushkevich, and Scatchard isotherm constants for adsorption of BER on the imprinted polymer (AD-10).

Langmuir isotherm	
Q_m (μmol/g)	21.39
K_L (L/mmol)	15.90
R^2	0.9978
Freundlich isotherm	
K_F (μmol/g)	46.61
b_F	0.5842
R^2	0.9764
Dubinin–Radushkevich isotherm	
Q_{DR} (μmol/g)	22.29
K (kJ^2/mol^2)	−0.0154
E (kJ/mol)	5.70
R^2	0.9785
Scatchard isotherm	
Q_{max} (μmol/g)	21.45
K_D (μmol/L)	65.80
R^2	0.9792

Note: R^2 is the correlation coefficient.

3.5. SPE specificity of the imprinted polymer

The imprinted and non-imprinted polymers (AD-10 and AD-B10) were employed as the adsorbents of the SPE column for the separation of BER and structurally similar PAL (Fig. 1) using HPLC analysis. Fig. 11 shows the percentages of the solutes eluted from a mixture of 0.1 mm BER and 0.1 mm PAL on SPE columns of AD-10 and AD-B10 with different eluting solutions of MeOH/$CHCl_3$ (v/v). The amounts of BER and PAL eluted from SPE column of AD-10 decreased from 17.9 to 1.0 and from 6.9 to 1.0 times, respectively, than those eluted from SPE column of AD-B10, as the ratio of MeOH/$CHCl_3$ (v/v) of eluting solutions increased from 0/1 to 1/10. The SPE column with AD-10 as the adsorbent and an eluting solution of 1/60 (v/v) MeOH/$CHCl_3$ showed that the adsorption of BER was 11.1 times higher than that of PAL. The two extra dimethoxy groups in PAL create a larger space volume than the methylenedioxy group in BER, and it is more difficult for PAL to embed into the cavity of the BER imprinted polymer, resulting in its easier elution. These results demonstrated that the AD-10 afforded more efficiency, and higher specificity and selectivity for the SPE of BER.

A real sample was prepared through a reflux extraction of the cortices of *P. wilsonii*, which were collected at the mountain (altitude of 2340 m) of Tu'uifeng, Nanto'ou Hsien, Taiwan, ROC, in methanol solvent for 5 h. Fig. 12 shows HPLC chromatographs of the methanol extract from the cortices of *P. wilsonii*. The methanol extract before SPE column of AD-10 appeared two peaks at 9.27

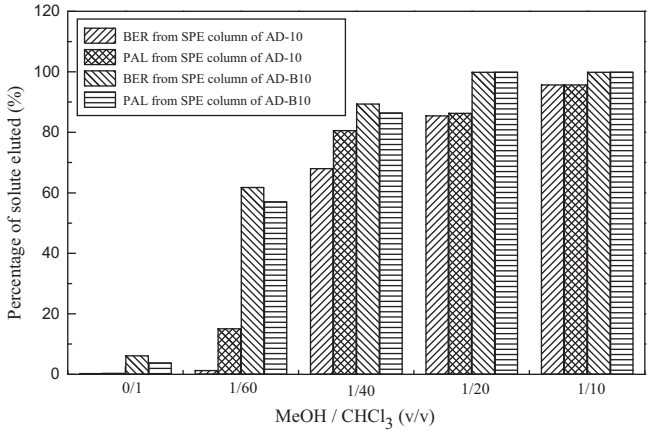

Fig. 11. Percentages of the solutes eluded from the mixture of 0.1 mm BER and 0.1 mm PAL on SPE columns of AD-10 and AD-B10 with different eluting solutions of MeOH/$CHCl_3$ (v/v).

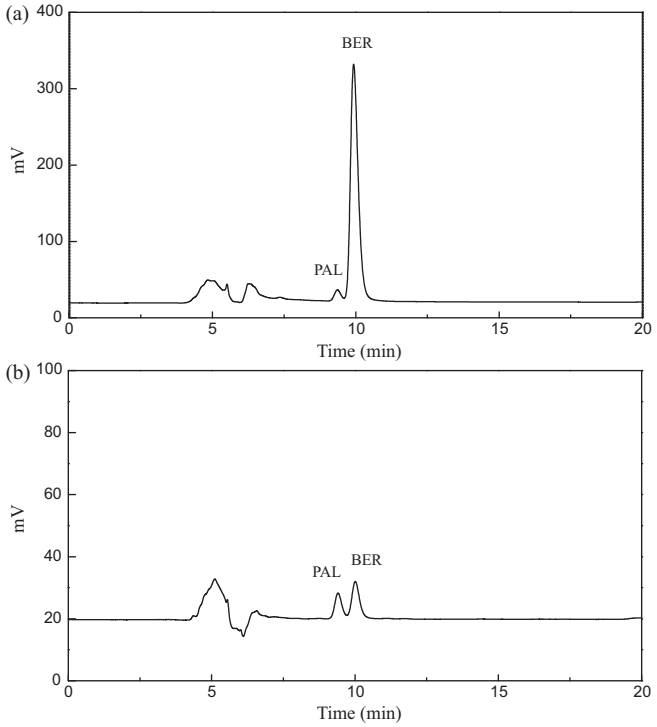

Fig. 12. HPLC chromatographs of the methanol extract from the cortices of *Phellodendron wilsonii*: (a) the solution of the methanol extract before SPE column of AD-10 and (b) the eluted solution of the methanol extract after SPE column of AD-10 by eluting with the mixture solution of MeOH and $CHCl_3$ (1/60, v/v).

and 9.93 min of retention times for PAL and BER, respectively, and the molar ratio of BER and PAL was 21.25 (Fig. 12(a)). However, the elution of the methanol extract using the SPE column with AD-10 in MeOH and $CHCl_3$ (1/60, v/v) showed that the molar ratio of BER and PAL significantly decreased to only 1.45 (Fig. 12(b)). About 96.10% of the BER in the methanol extract was adsorbed by AD-10, while only 39.24% PAL was adsorbed by the same column. Thus, AD-10 can be successfully used as an adsorbent for SPE in the determination of BER and its extraction from natural products.

4. Conclusion

Imprinted polymers were prepared using a non-covalent imprinting method with BER as the template, AA and MAA as the functional monomers, and EGDMA as the cross-linker (EGDMA) in three different porogens ($CHCl_3$, CH_3OH, and DMSO) with an initiator (AIBN) under 352 nm irradiation. The results showed that, compared to other imprinted polymers, AD-10 had not only a higher ratio of Q_{MIP}/Q_{BP} for the adsorption of BER, and but also a larger ratio of $Q_{MIP,B}/Q_{MIP,P}$ for the specificity and selectivity of adsorption of BER than structurally similar PAL. Spectrophotometric analysis demonstrated that a 1:1 cooperative hydrogen-bonding complex may predominate during pre-polymerization between the BER template and the AA monomer, which had a K_a of 6.35×10^3 L/mol. The adsorption experiments of BER on AD-10 were in accordance with the second-order and Langmuir adsorption models. The E value (5.70 kJ/mol) of BER, calculated from the Dubinin–Radushkevich model, indicated that adsorption proceeded via physisorption. The Scatchard plot of BER on AD-10 showed a single straight line with a K_D of 65.80 μmol/L. SPE analyses of a mixture of BER and PAL and methanol extract from the cortices of *P. wilsonii* showed that AD-10 had more efficiency, and higher specificity and selectivity for SPE of BER. The polymer can be successfully used as an adsorbent for SPE in the concentration and determination of BER and its extraction from natural products.

References

[1] F.G. Tamayo, E. Turiel, A. Martin-Esteban, J. Chromatogr. A 1152 (2007) 32–40.
[2] E. Turel, A. Martin-Esteban, Anal. Chim. Acta 668 (2010) 87–99.
[3] B. Sellergren, J. Chromatogr. A 906 (2001) 227–252.
[4] Q. Fu, H. Sanbe, C. Kagawa, K.K. Kunimoto, J. Haginaka, Anal. Chem. 75 (2003) 191–198.
[5] X. Huang, H. Zou, X. Chen, Q. Luo, L. Kong, J. Chromatogr. A 984 (2003) 273–282.
[6] M. Sibrian-Vazquez, D.A. Pivak, J. Am. Chem. Soc. 126 (2004) 7827–7833.
[7] R.J. Ansell, Adv. Drug Deliv. Rev. 57 (2005) 1809–1835.
[8] K. Haupt, K. Mosbach, Chem. Rev. 100 (2000) 2495–2504.
[9] L. Ye, K. Mosbach, J. Am. Chem. Soc. 123 (2001) 2901–2902.
[10] N.T. Greene, S.L. Morgan, K.D. Shimizu, Chem. Commun. (2004) 1172–1173.
[11] O. Ramstrom, K. Mosbach, Curr. Opin. Chem. Biol. 3 (1999) 759–764.
[12] G. Wulff, Chem. Rev. 102 (2002) 1–27.
[13] H.H. Yang, S.Q. Zhang, W. Yang, X.L. Chen, Z.X. Zhuang, J. Am. Chem. Soc. 126 (2004) 4054–4055.
[14] D. Cunliffe, A. Kirby, C. Alexander, Adv. Drug Deliv. Rev. 57 (2005) 1836–1853.
[15] J. Jodlbauer, N.M. Maier, W. Lindner, J. Chromatogr. A 945 (2002) 45–63.
[16] G. Theodoridis, A. Kantifes, J. Chromatogr. A 948 (2002) 163–169.
[17] G. Theodoridis, A. Kantifes, P. Manesiotis, N. Raikos, H. Tsoukai-Papadopoulou, J. Chromatogr. A 987 (2003) 103–109.
[18] X. Dong, W. Wang, S. Ma, H. Sun, Y. Li, J. Guo, J. Chromatogr. A 1070 (2005) 125–130.
[19] X. Zhu, Q. Cao, N. Hou, G. Wang, Z. Ding, Anal. Chim. Acta 561 (2006) 171–177.
[20] X. Song, J. Li, J. Wang, L. Chen, Talanta 80 (2009) 694–702.
[21] S. Scorrano, L. Longo, G. Vasapollo, Anal. Chim. Acta 659 (2010) 167–171.
[22] P. Lucci, D. Derrien, F. Alix, C. Perollier, S. Bayoudh, Anal. Chim. Acta 672 (2010) 15–19.
[23] L. Pan, Q. Tang, Q. Fu, B. Hu, J. Xiang, J. Qian, Acta Pharmacol. Sin. 26 (2005) 1334–1338.
[24] C.L. Kuo, C.W. Chi, T.Y. Liu, Cancer Lett. 203 (2004) 127–137.
[25] W. Kong, J. Wei, P. Abidi, M. Lin, S. Inaba, C. Li, Y. Wang, Z. Wang, S. Si, H. Pan, Nat. Med. 1012 (2004) 1344–1351.
[26] J. Yin, R. Hu, M. Chen, J. Tang, F. Li, Y. Yang, J. Chen, Metabolism 51 (2002) 1439–1443.
[27] C. Morel, F.R. Stermitz, G. Tegos, K.I. Lewis, J. Agric. Food Chem. 51 (2003) 5677–5679.
[28] M. Cernakova, D. Kostalova, Folia Biol. 47 (2002) 375–378.
[29] M.L. Freile, F. Giannini, G. Pucci, A. Sturniolo, L. Rodero, O. Pucci, V. Balzareti, R.D. Enriz, Fitoterapia 74 (2003) 702–705.
[30] Y. Tunc, N. Hasirci, A. Yesilada, K. Ulubayram, Polymer 47 (2006) 6931–6940.
[31] R.M. Silverstein, F.X. Webster, D.J. Kiemle, Spectrometric Identification of Organic Compounds, 7th ed., John Wiley & Sons, New York, 2005, pp. 72–126.
[32] G.P. Gonzalez, P.F. Hernando, J.S.D. Alegria, Anal. Chim. Acta 557 (2006) 179–183.
[33] I. Langumuir, J. Am. Chem. Soc. 40 (1918) 1361–1403.
[34] H.M.F. Freundlich, Z. Phys. Chem. A57 (1906) 358–471.
[35] S.P. Ramnani, S. Sabharwal, React. Funct. Polym. 66 (2006) 902–909.
[36] K.J. Shea, D.A. Spivac, B. Sellergren, J. Am. Chem. Soc. 115 (1993) 3368–3369.
[37] A.H. Chen, S.H. Chen, J. Hazard. Mater. 172 (2009) 1111–1121.
[38] A.H. Chen, Y.Y. Huang, J. Hazard. Mater. 177 (2010) 668–675.
[39] C.Y. Chen, J.C. Chang, A.H. Chen, J. Hazard. Mater. 185 (2011) 430–441.